

CHAPTER 4

RESULTS AND DISCUSSION

4.1. Preparation of tetracalcium phosphate

Results of the experiment were summarized in Table 4.1 and the patterns of XRD analysis were shown in Fig. 4.1, 4.2 and 4.3.

Table 4.1 Sintering conditions of the mixtures of DCPD and CaCO_3 in air for 6 hours.

No.	Sintering Conditions			X-ray diffraction results*
	Composition of mixture	Molar ratio	Temperature ($^{\circ}\text{C}$)	
1.	DCPD+ CaCO_3 (Stoichiometric)	1 : 1	1300	TTCP+HA , HA+TTCP
2.		1 : 1	1350	TTCP+HA,TTCP+ $\text{Ca}(\text{OH})_2$
3.		1 : 1	1400	TTCP+ $\text{Ca}(\text{OH})_2$
4.	DCPD+ CaCO_3	1 : 0.5	1350	α -TCP
5.		1 : 0.5	1400	α -TCP
6.	DCPD+ CaCO_3	1 : 0.8	1350	HA
7.		1 : 0.8	1400	HA
8.	DCPD+ CaCO_3	1 : 0.9	1350	TTCP,TTCP+HA + $\text{Ca}(\text{OH})_2$
9.		1 : 0.9	1400	TTCP+ $\text{Ca}(\text{OH})_2$, HA+TTCP
10.	DCPD+ CaCO_3	1 : 1.3	1350	TTCP+CaO
11.		1 : 1.3	1400	TTCP
12.		1 : 1.5	1400	TTCP+CaO
13.		1 : 2.3	1400	TTCP+CaO, $\text{Ca}(\text{OH})_2$

* In the case of mix phases , the first one was the main phase

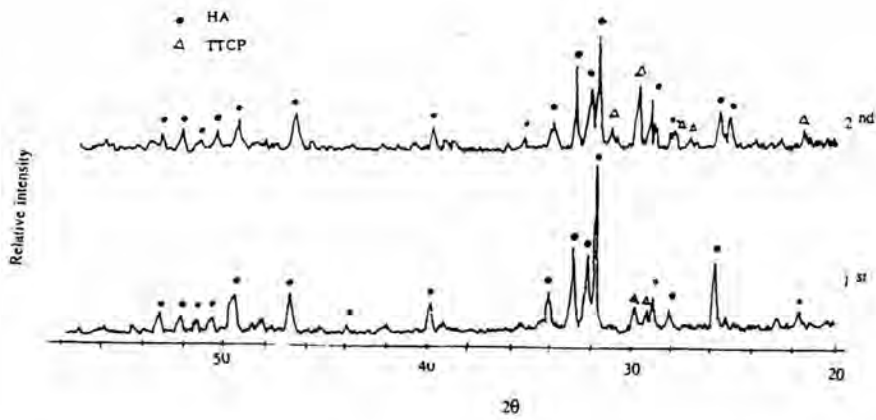


Fig. 4.1 XRD patterns of phase obtained after sintering the equimolar mixture of DCPD : CaCO_3 at 1300°C

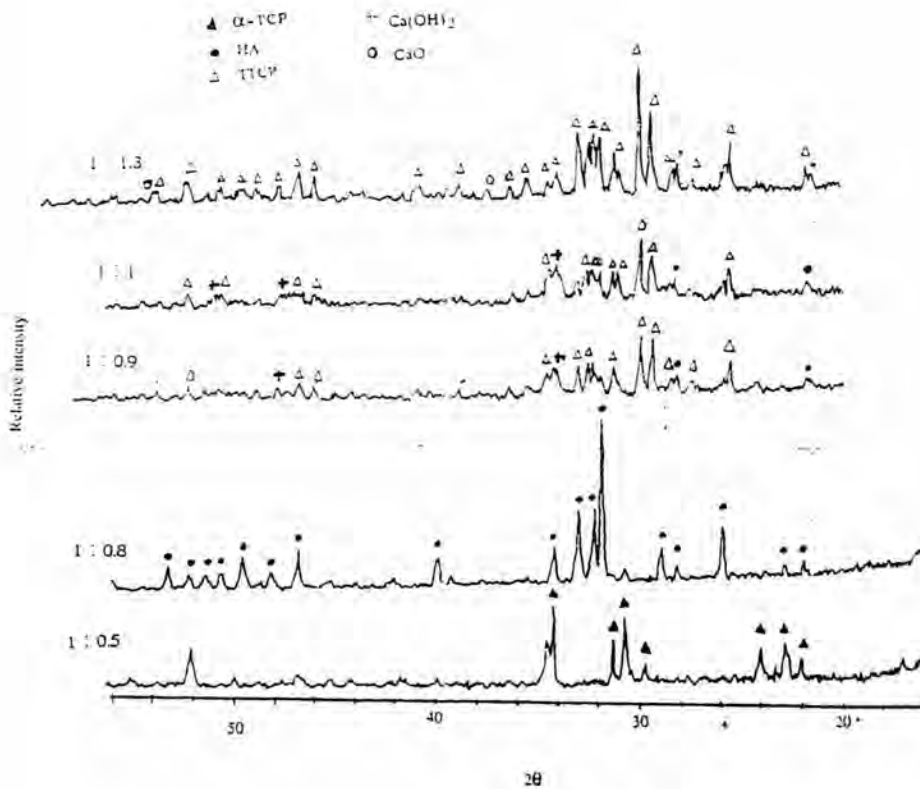


Fig. 4.2 XRD patterns of phase obtained after sintering the DCPD : CaCO_3 mixture of various molar ratios at 1350°C

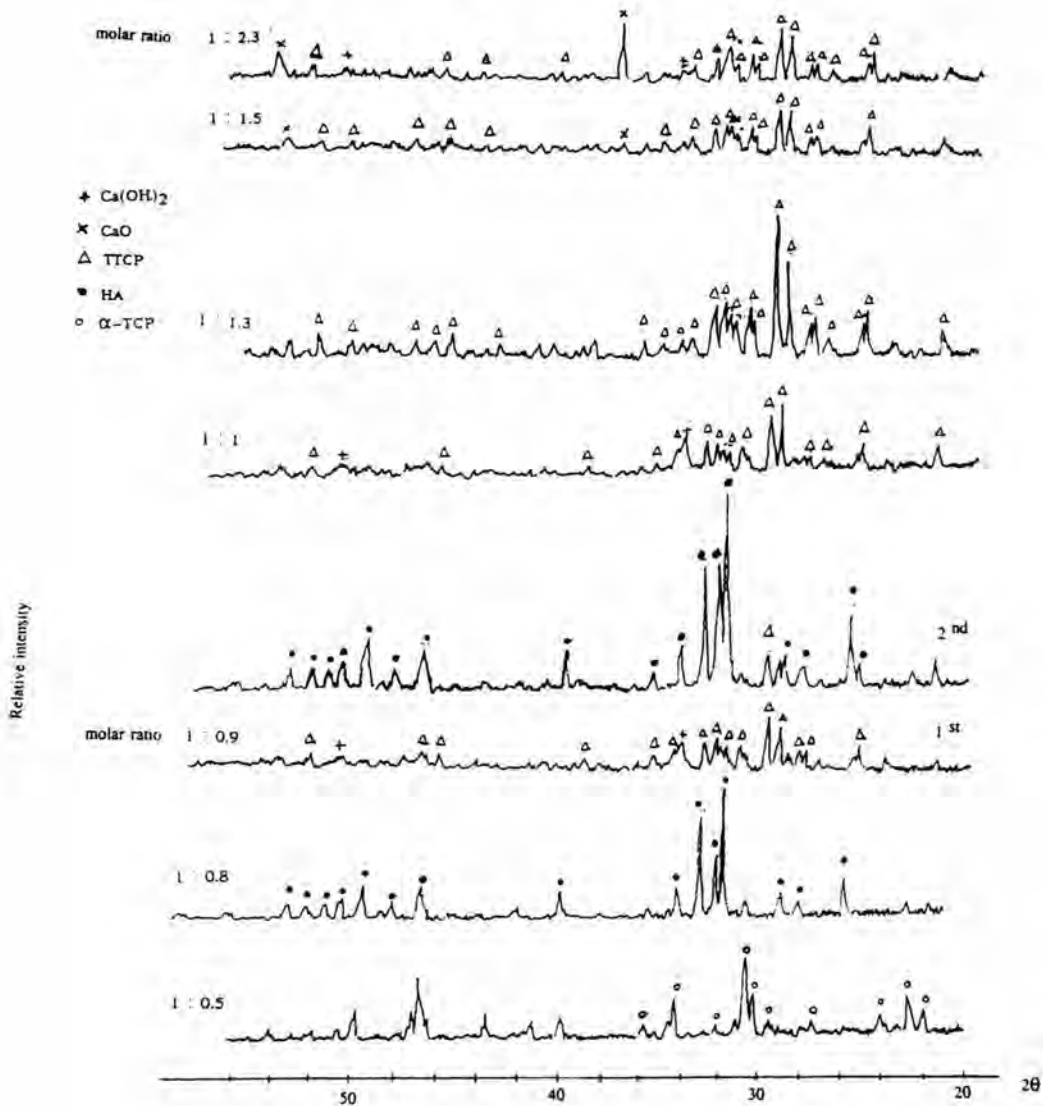


Fig. 4.3 XRD patterns of phase obtained after sintering the DCPD : CaCO_3 mixture of various molar ratios at 1400°C

The analysis by XRD of equimolar mixtures sintered at 1300°C (Fig. 4.1) showed the mixed phases between TTCP and HA and the instability of the major phase. Results of Fig 4.2 were the effect of molar ratio on the phase obtained at 1350°C . At low values (1:0.5, 1:0.8) single phase of α -TCP and HA were detected respectively and with increasing values (1:0.9, 1:1.0, 1:1.3), TTCP appeared as the main phase and also CaO was detected at the molar ratio of 1:1.3. At higher temperature (1400°C), single phase TTCP was produced at molar ratio of 1:1 but at higher molar ratios, 1:1.5 and 1:2.3, CaO and Ca(OH)_2 also appeared.

4.2 Sintering the mixture of γ - $\text{Ca}_2\text{P}_2\text{O}_7$ and CaCO_3

Results of the preparation of γ - $\text{Ca}_2\text{P}_2\text{O}_7$ from DCPD were tabulated in Table 4.2 and Fig 4.4. It was found from 400°C to higher temperature that β - $\text{Ca}_2\text{P}_2\text{O}_7$ was always present as a second phase and its content increased with temperature and at 350°C the dehydration of DCPD was not complete which was evident by the presence of CaHPO_4 ($d= 3.37, 2.96$).

Table 4.2 Phase analysis of the calcined DCPD at various temperatures

Temperature ($^\circ\text{C}$)	Phase present
350	CaHPO_4 + γ - $\text{Ca}_2\text{P}_2\text{O}_7$
400	γ - $\text{Ca}_2\text{P}_2\text{O}_7$ + β - $\text{Ca}_2\text{P}_2\text{O}_7$
410	γ - $\text{Ca}_2\text{P}_2\text{O}_7$ + β - $\text{Ca}_2\text{P}_2\text{O}_7$
440	γ - $\text{Ca}_2\text{P}_2\text{O}_7$ + β - $\text{Ca}_2\text{P}_2\text{O}_7$
500	γ - $\text{Ca}_2\text{P}_2\text{O}_7$ + β - $\text{Ca}_2\text{P}_2\text{O}_7$

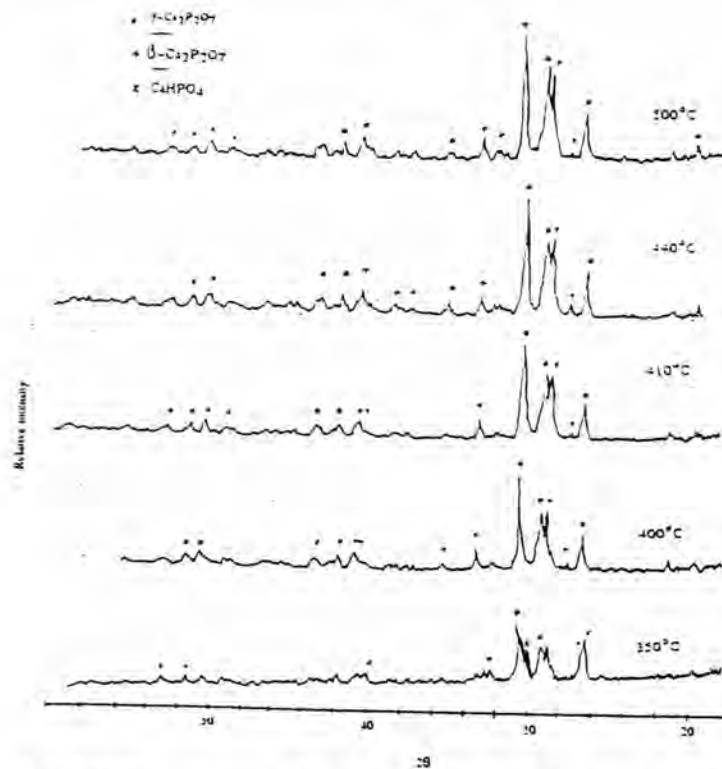


Fig. 4.4 XRD patterns of calcined DCPD at 350 – 500°C

The results of sintering of the mixtures of γ - $\text{Ca}_2\text{P}_2\text{O}_7$ and CaCO_3 were in Table 4.3, Fig. 4.5 and 4.6.

Table 4.3 Phase obtained from sintering the mixture of γ - $\text{Ca}_2\text{P}_2\text{O}_7$ + CaCO_3 (AR grade) in air for 6 hours.

No.	Sintering Conditions			X-ray diffraction results
	Composition of mixture	Molar ratio	Temperature ($^{\circ}\text{C}$)	
1.	γ - $\text{Ca}_2\text{P}_2\text{O}_7(500)$ + CaCO_3	2 : 3.0	1300	HA+TTCP(vs)
2.	γ - $\text{Ca}_2\text{P}_2\text{O}_7(500)$ + CaCO_3	2 : 3.5	1300	HA+TTCP+CaO(vs)
3.	γ - $\text{Ca}_2\text{P}_2\text{O}_7(440)$ + CaCO_3	2 : 3.8	1300	HA+TTCP(vs)+CaO(vs)
4.	γ - $\text{Ca}_2\text{P}_2\text{O}_7(440)$ + CaCO_3	2 : 4.0	1300	HA+TTCP(vs)+CaO(vs)
5.	γ - $\text{Ca}_2\text{P}_2\text{O}_7(410)$ + CaCO_3	2 : 3.8	1400	TTCP
6.	γ - $\text{Ca}_2\text{P}_2\text{O}_7(410)$ + CaCO_3	2 : 4.0	1400	TTCP

vs : very small

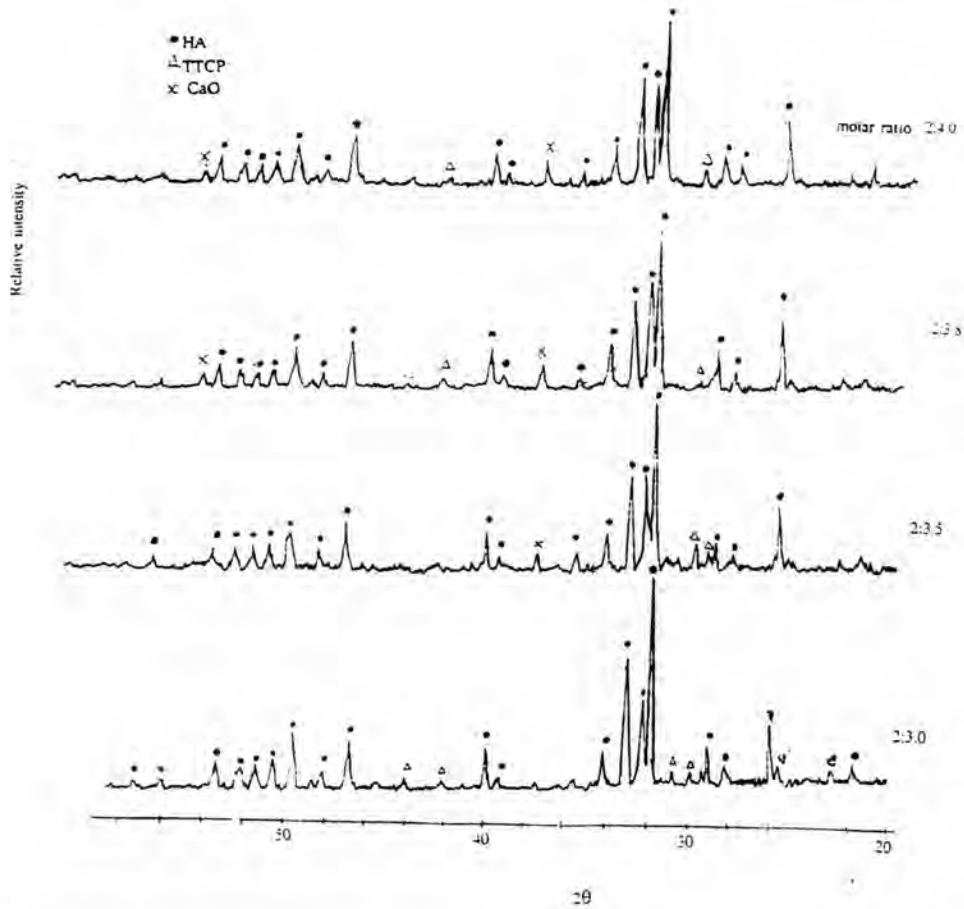


Fig. 4.5 XRD patterns of phases obtained after sintering the mixture of γ - $\text{Ca}_2\text{P}_2\text{O}_7(500)$ and CaCO_3 of molar ratio: a) 2:3 and b) 2:3.5 at 1300°C and the mixture of γ - $\text{Ca}_2\text{P}_2\text{O}_7(440)$ and CaCO_3 , with molar ratio: c) 2:3.8 and d) 2:4.0 at 1300°C

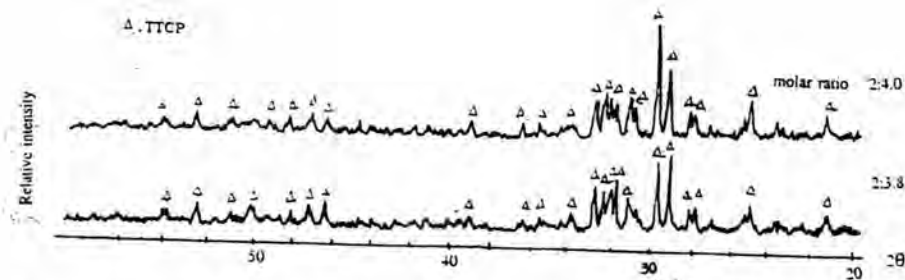


Fig. 4.6 XRD patterns of phase obtained after sintering the mixture of γ - $\text{Ca}_2\text{P}_2\text{O}_7(410)$ and CaCO_3 molar ratio : a) 2:3.8 b) 2:4.0 at 1400°C

Fig. 4.5, the XRD patterns of sintered γ - $\text{Ca}_2\text{P}_2\text{O}_7$ (500 and 440°C) + CaCO_3 mixtures of various molar ratios at 1300°C showed that HA was the main phase and some TTCP but when the value of molar ratio increased, CaO also appeared. Fig. 4.6 was the results at 1400°C which revealed the presence of single phase TTCP form the sintering of γ - $\text{Ca}_2\text{P}_2\text{O}_7$ (410°C) : CaCO_3 mixture of molar ratios 2:3.8 and 2:4.0. Table 4.4 was the summarized results of sintering of γ - $\text{Ca}_2\text{P}_2\text{O}_7$ (400) + CaCO_3 mixtures at 1350 and 1400°C.

Table 4.4 Phases obtained after sintering various mole ratio mixtures of γ - $\text{Ca}_2\text{P}_2\text{O}_7$ (400) and CaCO_3 in air at 1350°C and 1400°C for 6 hours

No.	Synthesis Conditions No.			X-ray diffraction results*
	Composition of mixture	Molar ratio	Temperature (°C)	
1.	γ - $\text{Ca}_2\text{P}_2\text{O}_7$ (400) + CaCO_3	2 : 3.0	1350	HA +TTCP
2.		2 : 3.5	1350	HA+TTCP
3.		2 : 3.8	1350	TTCP+HA
4.		2 : 3.9	1350	TTCP
5.		2 : 4.0	1350	TTCP
6.		2 : 4.3	1350	TTCP+Ca(OH) ₂
7.	γ - $\text{Ca}_2\text{P}_2\text{O}_7$ (400) + CaCO_3	2 : 3	1400	HA+TTCP
8.		2 : 3.5	1400	HA+TTCP
9.		2 : 3.8	1400	TTCP+HA
10.		2 : 4.0	1400	TTCP
11.		2 : 4.3	1400	TTCP+CaO
12.		2 : 4.8	1400	TTCP+Ca(OH) ₂ +CaO

* The first one was the main phase.

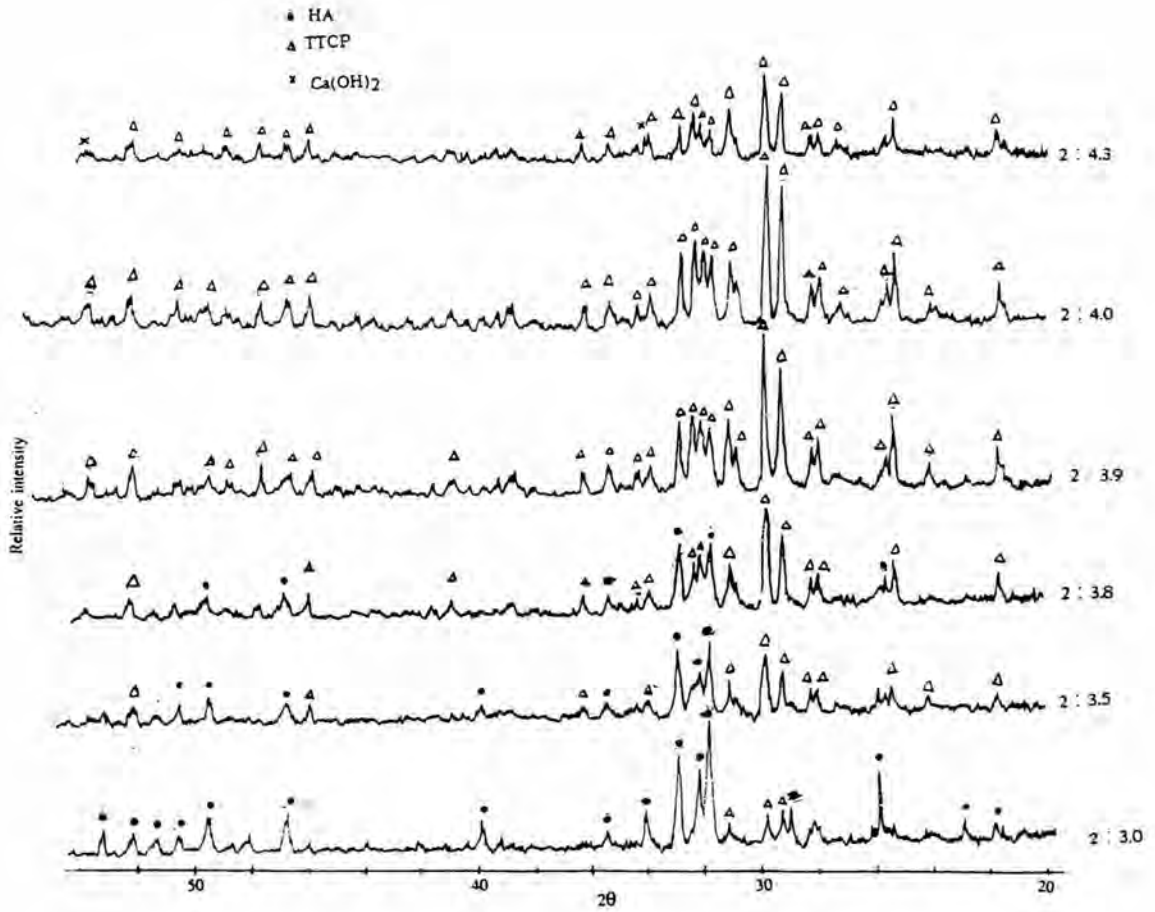


Fig. 4.7 XRD patterns of phases obtained after sintering the mixture of γ -Ca₂P₂O₇(400) and CaCO₃ of various molar ratios at 1350°C

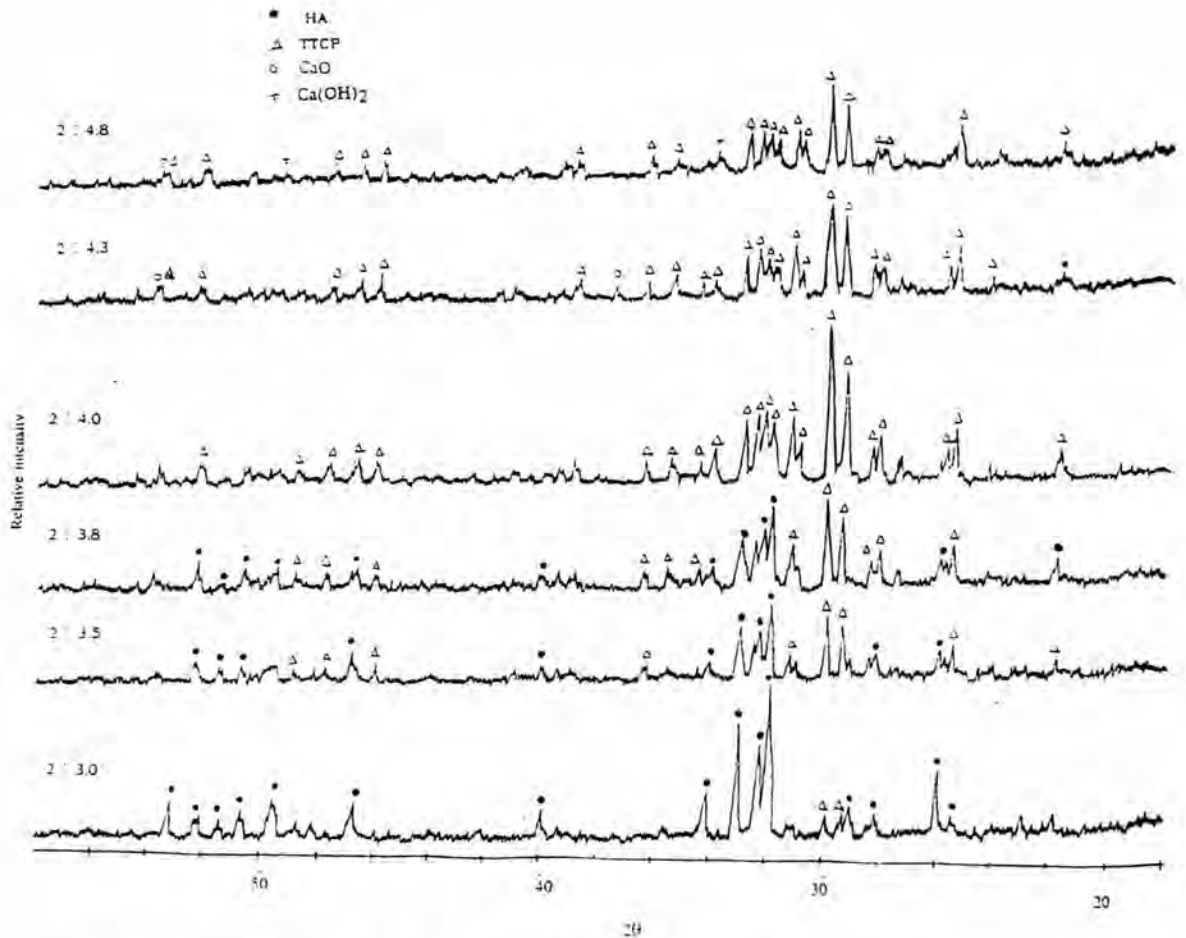


Fig. 4.8 XRD patterns of phases obtained after sintering the mixture of γ - $\text{Ca}_2\text{P}_2\text{O}_7(400)$ and CaCO_3 of various molar ratios at 1400°C

Results of Table 4.4 gave the same trend as that of Table 4.3 in that when the molar ratio of the mixture was raised close to 2:4.0, content of TTCP increased and single phase TTCP was also found at 2:4.0. When the molar ratio far exceeded 2:4.0, i.e. at 2:4.3, Ca(OH)_2 ($d=2.628, 1.927$) was noticed (Fig.4.7). Fig. 4.8 also gave the same trend as the previous ones.

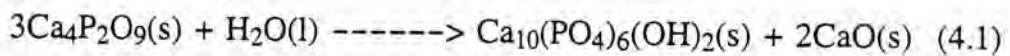
In conclusion, the two methods (4.1 and 4.2) could produce single phase TTCP at temperature $1350\text{--}1400^\circ\text{C}$. When using the stoichiometric

mixtures and at higher temperature (1400°C), the reproducibility with γ -Ca₂P₂O₇ method was better. Which was in agreement with the reactions in equations 2.11, 2.12, 2.13 and 2.17. At 1300°C, the water vapor in the furnace atmosphere favored the formation of HA and at an elevated temperature, i.e. 1400°C, the equilibrium of the reaction 2.13 was shifted to the right, hence metastabilized tetracalcium phosphate.

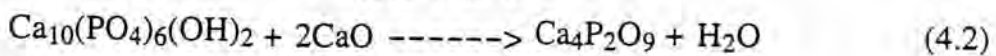
Phase diagram of CaO/P₂O₅ mixture, Figure 1.1 and 1.2, showed the influence of partial vapor pressure on the stability of various calcium phosphate as a function of temperature.

At 1300°C it was found that the content of HA increased because water vapor in air leading to the formation of hydroxyapatite (eq. 2.11, 2.12, 2.13). When the annealing temperature was elevated from 1300 to 1400°C the equilibrium of reversible reaction (2.13) was shifted to the right side. It was possible to obtain the single phase of tetracalcium phosphate.

Ciesla and Rudnicki (1987) reported that during heating tetracalcium phosphate in the air at temperature from 400 to 1100°C, reaction with water vapor and carbon dioxide took place at the temperature higher than 660°C. The products of the reaction were : stoichiometric calcium hydroxyapatite and CaO, the reaction running according to



1200-1400°C



Under carbon dioxide atmosphere, at temperature higher than 480°C tetracalcium phosphate was transformed into carbonate apatite AB.

According to what having been described, the condition : 2:4.0 molar ratio of γ -Ca₂P₂O₇(400°C) : CaCO₃ mixture sintering at 1400°C was chosen to produce TTCP for the preparation of calcium phosphate cement.

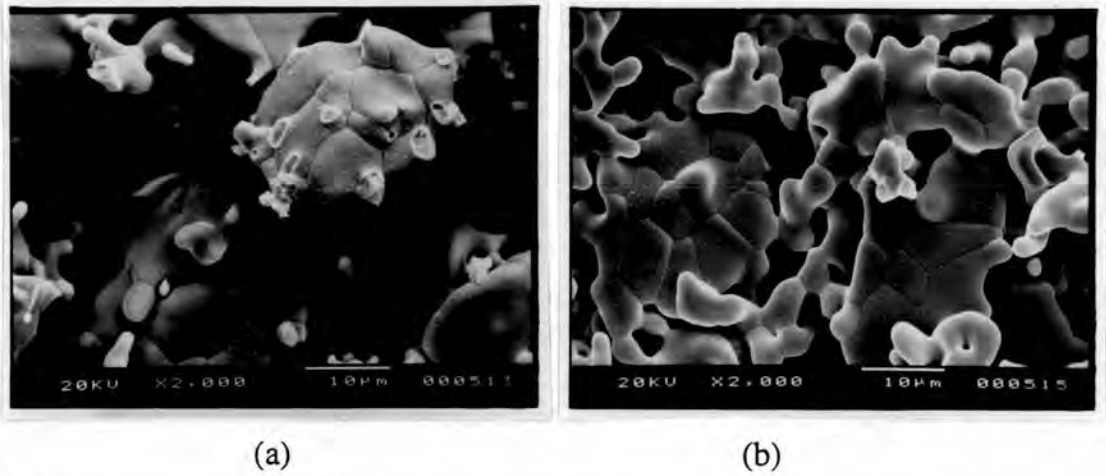


Fig. 4.9 SEM micrographs of TTCP prepared by sintering the mixture of γ - $\text{Ca}_2\text{P}_2\text{O}_7(400)$ and CaCO_3 of molar ratio 2:4 : a) at 1350°C
b) at 1400°C

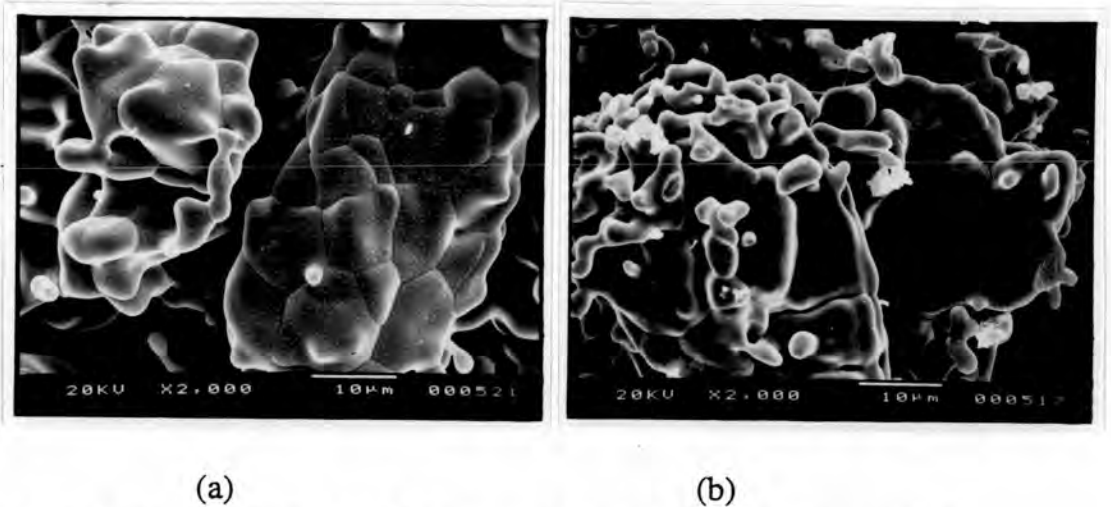


Fig. 4.10 SEM micrographs of TTCP prepared by sintering the mixture of DCPD and CaCO_3 : a) molar ratio 1:0.9 at 1400°C ; b) molar ratio 1:1.3 at 1350°C

Fig. 4.9 and 4.10 were the micrographs from SEM showing the extent of sintering, shape and size of grains of synthesized TTCP. The estimated grain diameter was about 10 μm .

Table 4.5 showed the chemical analysis of the prepared TTCP determined by ICP method.

Table 4.5 Chemical analysis of the prepared TTCP

Element (ppm)	MgO 0.4	Zn 65	Cu 8	Mn <0.4
	Al 0.02	V <3	Hg <1	Cr <5
	As 0.05	Ni <0.4	Bi <5	Cd <0.5
Ca : P	41.24% : 16.16% = 1.97 : 1 mole			

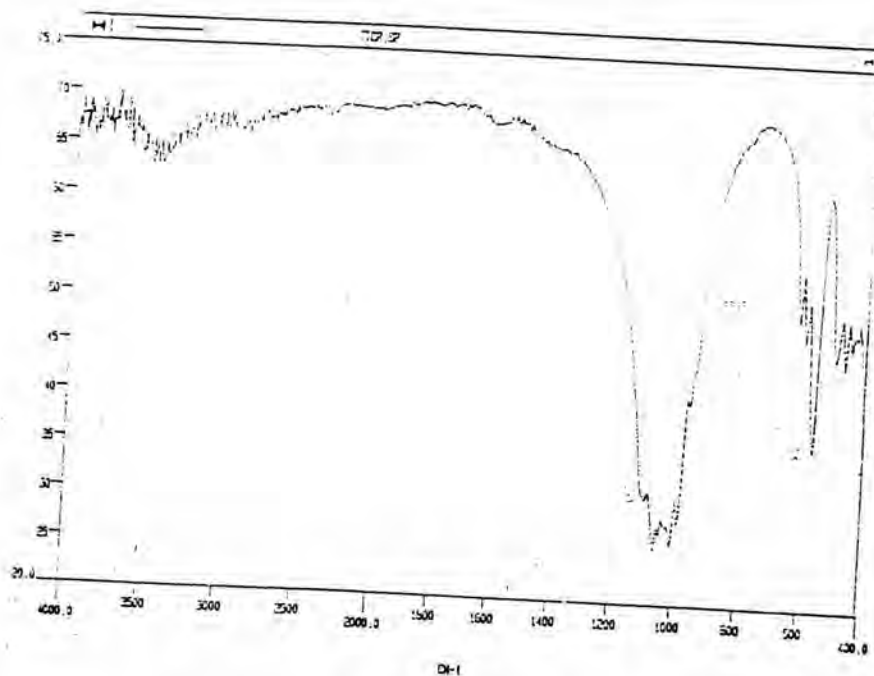


Fig. 4.11 IR spectra of the prepared TTCP

The results of chemical analysis of TTCP revealed the traces of impurities which were lower than the limit allowed according to ASTM F 1185-88 (standard specification for composition of ceramic hydroxyapatite for surgical implants) and the Ca/P molar ratio was nearly close to 2:1 of TTCP. The results of XRD, chemical analysis and IR confirmed that the prepared material was TTCP.

4.3 Preparation of calcium phosphate cement systems containing TTCP and DCPD.

(a) Setting time of cements.

The effect of HA as seed on setting time was tabulated and illustrated in Table 4.6, Fig. 4.12.

Table 4.6 Effect of content of HA(70) seed on the setting time of cements(TTCP(1350)+DCPD) (BET specific surface area of TTCP=1.06±0.01 m²/g) at P/L = 1.7 g/ml

No.	Content of HA (%)	Setting time (min)*		Phase present# (1 day)
		Initial	Final	
1.	0	19.5±3.8	>60	HA+TTCP+CaHPO ₄
2.	10	26.3±4.2	>60	HA+TTCP+CaHPO ₄
3.	15	27.0±2.6	>60	HA+TTCP+CaHPO ₄
4.	20	32.7±4.0	54.0±6.2	HA+TTCP+CaHPO ₄
5.	25	16.3±2.1	34.3±3.5	HA+TTCP+CaHPO ₄
6.	30	9.0±1.0	34.7±3.0	HA+TTCP+CaHPO ₄
7.	35	14.7±4.2	55.0±2.6	HA+TTCP+CaHPO ₄
8.	40	15.0±3.0	41.3±5.1	HA+TTCP+CaHPO ₄
9.	45	10.0±1.0	58.3±4.0	HA+TTCP+CaHPO ₄
10.	50	5.0±1.0	56.0±3.6	HA+TTCP+CaHPO ₄

* the number of each sample specimens is 3 ; # The first one was the main phase.

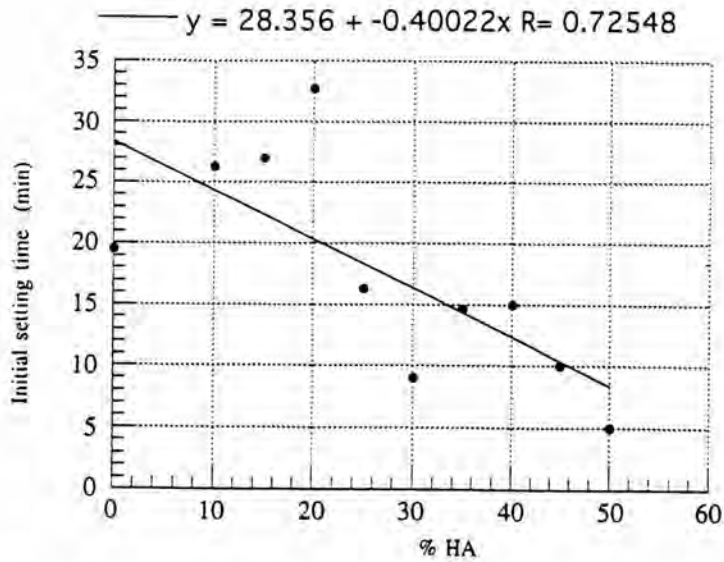


Fig. 4.12 The relationship between initial setting time and the content of HA(70) of TTCP+DCPD cement at 1.7 g/ml.

Fig. 4.12 was the plot between wt% HA and initial setting time (min) of cements. It was found from the plot that initial setting time of the cement could be controlled to meet requirement of a clinical application by adjusting the content of seed and also the P/L ratio used. As also shown in Table 4.6, the content of HA affected the final setting time as well.

Table 4.7 Setting time of cements containing the mixture of TTCP (1350 and 1400°C) and DCPD with HA(70) and CHA(70) as seeds at P/L ratio, of 2.4 g/ml (specific surface area(SS) of TTCP = 1.06 ± 0.01 m²/g, SS of HA(70) = 140.15 ± 4.20 m²/g, SS of CHA(70) = 83.21 ± 0.19 m²/g)

Calcium phosphate cement	% seed	Setting time (min) *		Phase (1 day)
		Initial	Final	
TTCP(1350)+DCPD	35%HA	9.0 \pm 1.0	41.0 \pm 3.6	HA +TTCP+CaHPO ₄
	40%HA	7.3 \pm 1.1	25.3 \pm 2.5	HA +TTCP+CaHPO ₄
	35%CHA	8.7 \pm 0.6	30.0 \pm 1.0	HA +TTCP+CaHPO ₄
	40%CHA	5.3 \pm 0.6	14.3 \pm 1.5	HA +TTCP+CaHPO ₄
TTCP(1400)+DCPD	35%HA	5.6 \pm 1.5	30.0 \pm 1.0	HA +TTCP+CaHPO ₄
	40%HA	8.0 \pm 1.0	29.0 \pm 1.7	HA +TTCP+CaHPO ₄
	35%CHA	8.0 \pm 2.0	29.3 \pm 5.8	HA+CaHPO ₄ (trace)
	40%CHA	7.0 \pm 1.0	12.6 \pm 2.5	HA+CaHPO ₄ (trace)

HA : Hydroxylapatite synthesised from cattle bone , CHA : Hydroxylapatite synthesised from pure chemical

* the number of each sample specimen was 3

Table 4.7 showed that when the content of HA seed increased, the setting time gradually reduced and comparison of the addition of HA seed with that of CHA suggested that the latter was a better accelerator. The effect of seed size as shown in Table 4.8.

Table 4.8 showed that unsieved HA gave a much shorter initial setting time. Therefore the particle size of seed also affected the setting time of CPC cement which was confirmed by the better crystallinity of HA formed (Fig. 4.27 d)

Table 4.8 Effect of particle size of HA(70) as seed on the setting time*(min) of cement (35,45wt% of HA,SS of TTCP(1350) = 1.06 ± 0.01 m²/g, P/L ratio of 1.7 g/ml)

HA size	%HA	35 wt% HA		45 wt% HA	
		Initial	Final	Initial	Final
-325 mesh		25	56	18	68
unsieved		10	56	11	59

Table 4.9 Effect of specific surface area of TTCP(1350^oC) on the setting time of calcium phosphate cement(TTCP+DCPD) added 40 wt% of HA(70) at P/L ratio of 2.0 g/ml.

Specific surface area of TTCP(1350) ,m ² /g	Setting time (min)*		Phase present in 1 day [#]
	Initial	Final	
0.95 \pm 0.02	13	57	HA+TTCP+CaHPO ₄ (trace)
1.06 \pm 0.01	19	99	HA+TTCP+CaHPO ₄ (trace)
1.40 \pm 0.04	13	64	HA+TTCP+CaHPO ₄ (trace)
1.53 \pm 0.04	12	38	HA+TTCP+CaHPO ₄ (trace)
1.63 \pm 0.01	10	33	HA+TTCP+CaHPO ₄ (trace)

* The number of each sample specimen was 3-5 , [#] XRD patterns showed in Fig. 4.28.

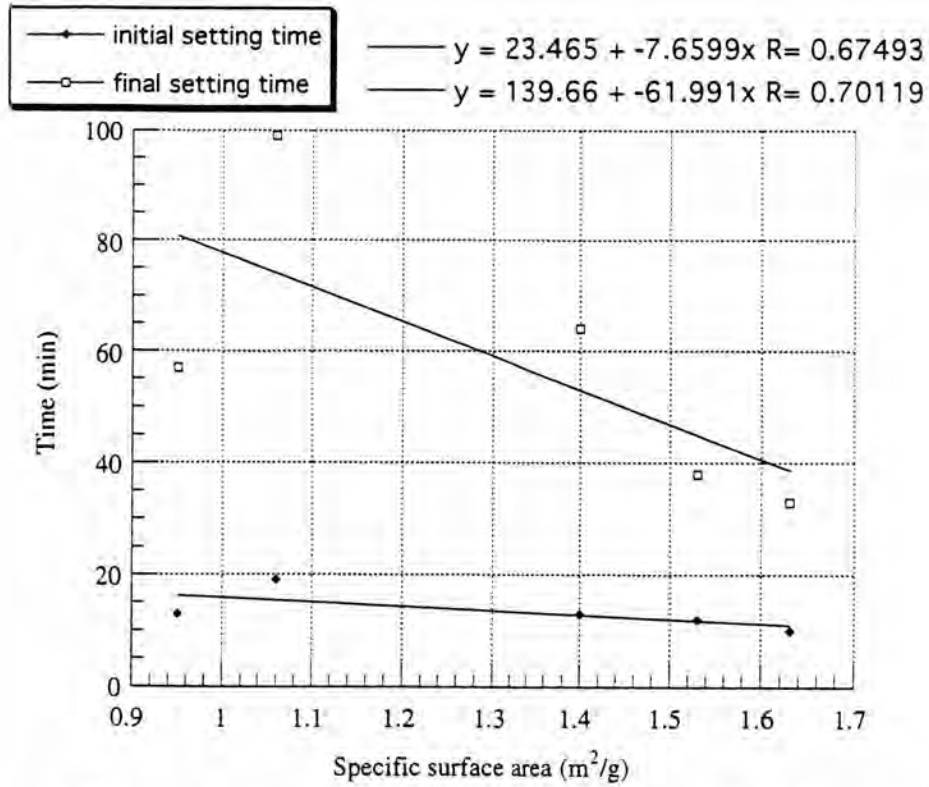


Fig. 4.13 The relationship between setting time and specific surface area of TTCP

Table 4.9, Fig 4.13 showed that the setting time of cements was reduced with increasing specific surface area of TTCP (small particle size). The initial setting time of cement containing large specific surface area of TTCP (1.63 ± 0.01 m²/g) was 10 min at P/L ratio of 2.0 g/ml.

Table 4.10 Effect of P/L ratio on the setting time of cement pastes containing the equimolar mixture of TTCP(1350) and DCPD in the absence and presence of seed

(SS of TTCP = $1.06 \pm 0.01 \text{ m}^2/\text{g}$)

Content of HA(70) (%)	P/L ratio	Setting time (min) *		Phase present (1 day)
		Initial	Final	
0	1.33	33.3 \pm 3.0	46.0 \pm 4.0	HA+TTCP+CaHPO ₄ (trace)
0	1.5	19.7 \pm 6.5	37.7 \pm 4.7	HA+TTCP+CaHPO ₄ (trace)
0	1.7	19.5 \pm 3.8	50.7 \pm 7.2	HA+TTCP+CaHPO ₄ (trace)
0	2.0	11.6 \pm 3.0	35.3 \pm 2.5	HA+TTCP+CaHPO ₄ (trace)
0	2.4	18.3 \pm 6.5	42.3 \pm 2.5	HA+TTCP+CaHPO ₄ (trace)
35	2.4	9.0 \pm 1.0	41.0 \pm 3.6	HA+TTCP+CaHPO ₄ (trace)
40	2.4	7.3 \pm 1.1	25.3 \pm 2.5	HA+TTCP+CaHPO ₄ (trace)

* the number of each sample specimens was 3.

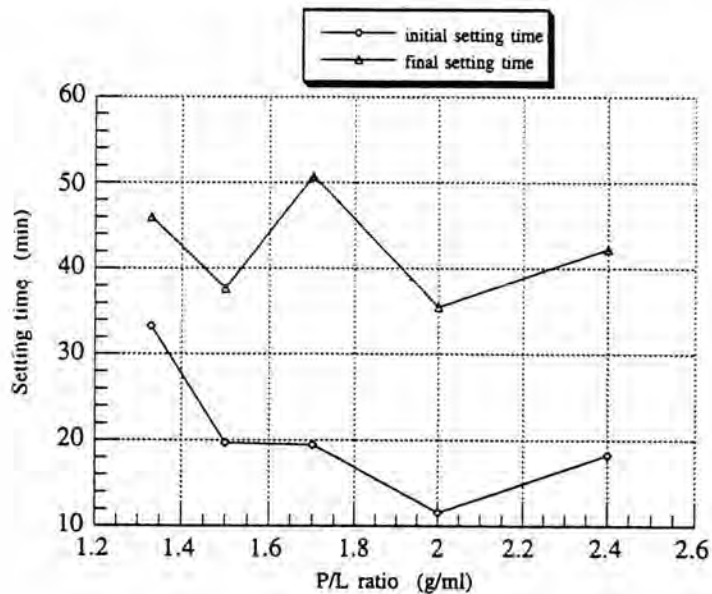


Fig. 4.14 the relationship between P/L ratio of pastes cement (TTCP(1350)+DCPD without seed) and setting time

Table 4.10 and Fig 4.14 showed that the trend of setting time was gradually reduced with the increasing of P/L ratio.

(b) Compressive strength of cements

Table 4.11 Effect of the content of hydroxyapatite on the compressive strength of cement containing the equimolar mixture of TTCP(1350°C) and DCPD. (BET specific surface area of TTCP(1350°C) $1.63 \pm 0.01 \text{ m}^2/\text{g}$)

% HA(70)	P/L	Compressive strength (MPa) 5 test pieces	Phase* (1 day)
0	2.0	0.23±0.1	HA+TTCP+CaHPO ₄
0	2.4	0.49±0.05	HA+TTCP+CaHPO ₄
10	2.0	0.45±0.1	HA+TTCP+CaHPO ₄
10	2.3	0.47±0.08	HA+TTCP+CaHPO ₄
10	2.4	0.53±0.02	HA+TTCP+CaHPO ₄
20	2.0	0.64±0.06	HA+TTCP+CaHPO ₄
20	2.4	0.65±0.1	HA+TTCP+CaHPO ₄
30	2.0	0.72±0.05	HA+TTCP+CaHPO ₄
30	2.4	0.56±0.05	HA+TTCP+CaHPO ₄
35	2.0	0.96±0.08	HA+TTCP+CaHPO ₄
35	2.4	0.60±0.05	HA+TTCP+CaHPO ₄
40	2.0	0.86±0.1	HA+TTCP+CaHPO ₄
40	2.4	0.47±0.1	HA+TTCP+CaHPO ₄

*The first one was the main phase. XRD patterns shown in Fig. 4.23.

Table 4.11 showed that, regardless of P/L ratio, the compressive strength of the cements increased with the content of seed up to 35 wt% HA and there was a slight decline in compressive strength at 40 wt% HA. Fig. 4.15 and 4.16 showed a sharp decline in the compressive strength of the

cements when the P/L ratio increased from 2.0 to 2.4. This was due to incomplete hydration caused by insufficient liquid.

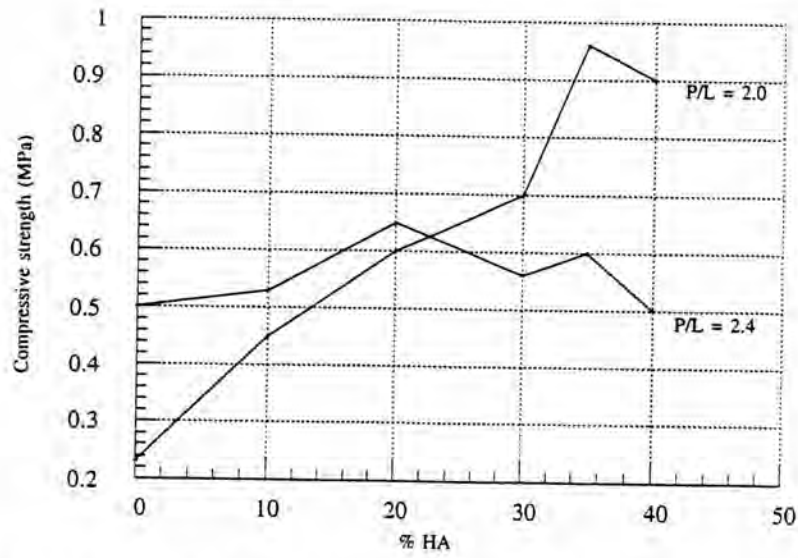


Fig. 4.15 change of 1 day compressive strength of cement containing TTCP(1350)+DCPD with the content of HA(70) as seed at P/L ratios of 2.0 and 2.4 g/ml. (curing at 80% humidity)

Table 4.12 Effect of HA(70) content on compressive strength (MPa) of cement containing the equimolar mixture of TTCP(1350), TTCP(1400) and DCPD at P/L ratio of 2.0 g/ml

%HA	0	10	20	30	35	40
TTCP						
prepared at 1350°C	0.23±0.1	0.45±0.1	0.64±0.06	0.72±0.05	1.0±0.08	0.89±0.1
prepared at 1400°C	-	-	0.60±0.1	0.70±0.2	0.8±0.08	0.70±0.05

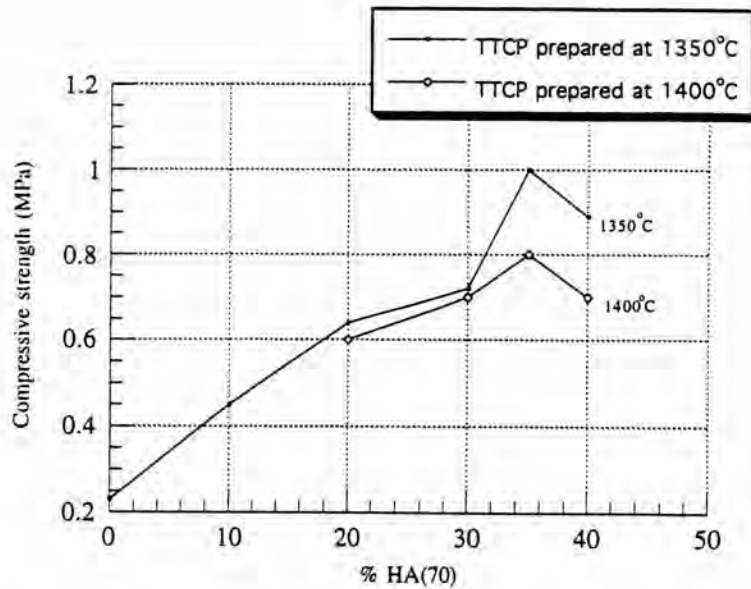


Fig. 4.16 One day compressive strength of cement containing TTCP(1350) and TTCP(1400), P/L = 2.0 g/ml. (curing at 80 %humidity)

Table 4.12 and Fig. 4.16 showed the effect of content of hydroxyapatite seed on the compressive strength of cements containing TTCP prepared at 1350 and 1400°C. It was found that both cements (P/L ratio of 2.0 g/ml) also had the maximum strength at 35 wt% HA which probably due to the formation of a better HA as hydration product at 35–40 wt% seed (Fig. 4.23).

Table 4.13 Compressive strength of CPC (TTCP(1350)+DCPD) specimens in the presence of 35, 40 wt% HA(70) at 1 and 7 day curings, P/L ratio of 2.0 g/ml. (SS of HA(70) = 140.15 m²/g, SS of TTCP = 1.63 m²/g)

% seed	Compressive strength(MPa) 5 specimens		Phase present*	
	1 day	7 days	1 day	7 days
35%HA(70)	1.0 \pm 0.08	0.67 \pm 0.2	HA+TTCP+CaHPO ₄	HA+TTCP+CaHPO ₄
40%HA(70)	0.89 \pm 0.1	0.52 \pm 0.1	HA+TTCP+CaHPO ₄	HA+TTCP+CaHPO ₄

* The first one was the main phase.

From Table 4.13, the compressive strength of CPC specimens at 1 day was higher than those of CPC specimens at 7 days in the presence of 35,40 wt% of HA. The compressive strength dropped from 1.0 \pm 0.08 MPa to 0.67 \pm 0.20 MPa in the presence of 35 wt% of HA and from 0.89 to 0.52 MPa in the presence of 40 wt% of HA. Fukase et al. (1990) reported the same phenomenon that the compressive strength at 24 h was lower than at 4 h, but the author did not discuss it. Liu et al. (1997) also reported that the mechanism of hardening process might explain this phenomenon.

However, Brown et al. (1991) found that a shell of HA was formed around the reactants, the rate of HA formation was controlled by the transport of water and ions through such a shell and decreased with an increase of the thick HA shell. The hydration of residual DCPA engulfed by the shell of HA would lead to an internal force which would be harmful to the compressive strength. Thus, the compressive strengths decreased with the process of hydration at the later stage.

Table 4.14 Effect of the addition of HA prepared at 70, 550 and 1280°C on the compressive strength of calcium phosphate cement (SS of TTCP = 1.63 m²/g)

% seed	Compressive strength (MPa) 1 day	Phase present* 1 day
35%HA(70)	1.00±0.08	HA+TTCP+CaHPO ₄
40%HA(70)	0.89±0.10	HA+TTCP+CaHPO ₄
35%HA(550)	0.54±0.07	HA+TTCP+CaHPO ₄
35%HA(1280)	0.22±0.02	HA+TTCP+CaHPO ₄
35%CH(550)	0.32±0.02	HA+TTCP+CaHPO ₄

* The first one was the main phase

Table 4.14 showed that in the presence of 35 wt% of HA prepared at 70°C had the highest compressive strength (1.0 MPa), hence the lower temperature HA was more effective as strength accelerator than higher temperature HA. This probably was due to the crystallinity of the seed HA which from XRD results, Fig 3.10, a, b and c of HA prepared at 70, 550 and 1280°C, respectively, it was found that the crystallinity of HA was high with the increasing of temperature. The specimens prepared from the mixture containing highly crystalline HA seeds also had high crystallinity but low compressive strength (0.2 MPa) as comformed with Takezawa et al. (1987)'s report.

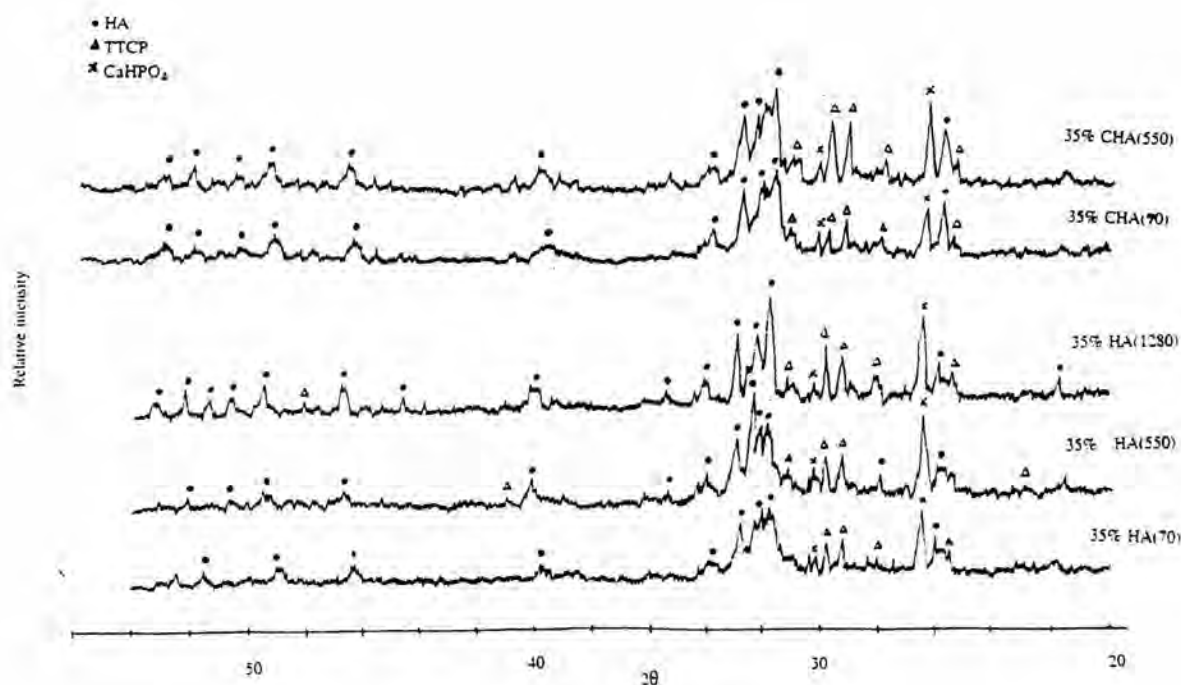


Fig. 4.17 XRD patterns of cement containing HA prepared at 70, 550 and 1280°C and of cement containing CHA prepared at 70 and 550°C, P/L ratio of 2.0, 1 day curing.

Fig 4.17 also confirmed that the cement containing 35 wt% HA(1280) and CHA (550) had a better crystallinity when compared to that of HA(70 and 550). Doi. et al. (1989) reported that the compressive strength of the set cements strongly depended on the types of HA added. The compressive strength of the cements containing HA prepared at temperatures higher than 60°C gradually weakened as HA preparation temperature increased and the compressive strength of the HA(100) cement was about one-fourth that of the HA(40) in nearly all direction. In the latter cement, needle-like HA and new apatite formed on HA crystals were entangled and intermeshed. With large HA crystals as seed it was likely that there were less chances for entanglement and intermesh; resulting in relatively a weak hard mass. Specific surface area of HA(550) was less than HA(70). Therefore, a similar conclusion was also obtained. However, the effect of HA crystallinity on cement strength might be offset by other factors.

Table 4.15 Effect of seed content on compressive strength of the pressed cement specimens containing the equimolar mixture of TTCP(1350°C) and DCPD at P/L ratio = 2.4 g/ml, 353.36 kg/cm²

(SS of TTCP = 1.06±0.01 m²/g, SS of HA(70) = 140.15 m²/g,

SS of CHA(70) = 83.21 m²/g)

% seed	Compressive strength (MPa)	phase present by X-ray diffraction *	
		1 day	1 month
35%HA	16.2±3.0	HA+TTCP+CaHPO ₄	HA+TTCP+CaHPO ₄
40%HA	6.9±1.6	HA+TTCP+CaHPO ₄	HA+CaHPO ₄
35%CHA	12.8±1.7	HA+TTCP+CaHPO ₄	HA+TTCP+CaHPO ₄
40%CHA	5.4±1.5	HA+TTCP+CaHPO ₄	HA+CaHPO ₄

* The first one was the main phase as shown in Fig. 4.18.

When specimens were pressed at 353.36 kg/cm², the compressive strength increased from 1.00±0.08 MPa to 16.2±3.0 MPa for cement containing 35 wt% of HA(70) as seed (Table 4.11 and 4.15) and was higher than cement containing 35 wt% CHA(70).

During hydration, the pore space in the hardened cement body was filled with hydrates, and the body was strengthened. There were many reports on the relationships between strength and pore volume. For example, Granju and Maso (1984) found that the compressive strength of hardened cement pastes had a close relationship, expressed by Ryshkewitch 's equation, with capillary porosity, not with total porosity. Takahashi. et al. (1997) reported the application of Griffith' s theory to the relationship between the compressive strength and porosity of hardened cement pastes. They showed that the water/cement ratio significantly affected these relationships

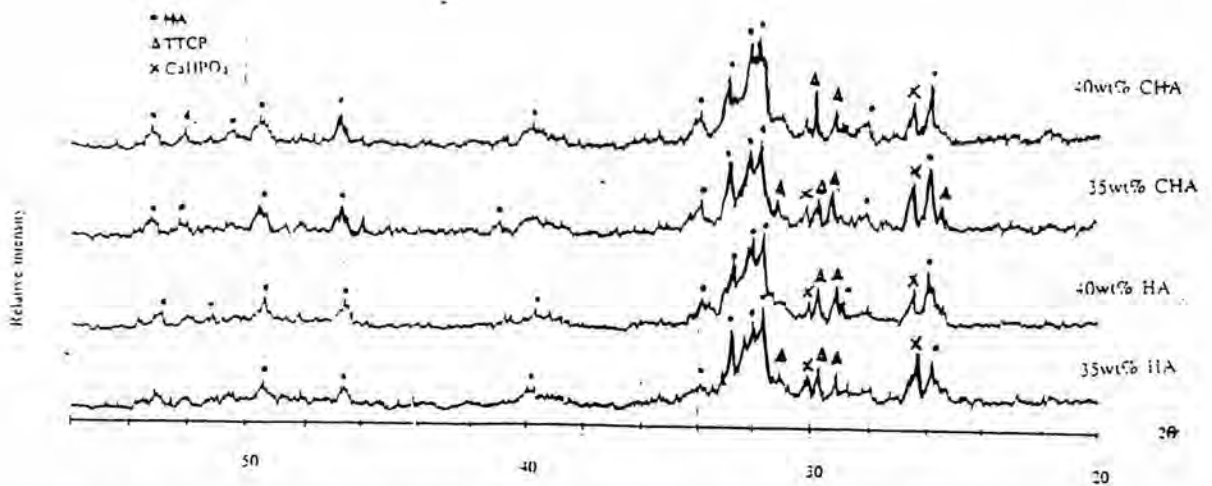


Fig. 4.18 Comparison of XRD patterns of cements added 35,40wt% HA(70) with that of cement added 35,40wt% CHA(70) (Table 4.15)

It was possible that pressing the specimens could reduce porosity of hardened cement pastes and affected the reducing of compressive strength. Because of a better in crystallinity of CHA, it was possible that the compressive strength of cement containing CHA as seed was lower. Phase obtained after 1 day was HA, unreacted TTCP and CaHPO_4 . The longer curing (1 month) time was, the more content of HA formed.

Table 4.16 Effect of SS of TTCP on the compressive strength of cement (TTCP(1350)+DCPD added 35 wt% HA(70)), P/L ratio of 2.0 g/ml.

BET specific surface area of TTCP(1350°C), m^2/g	Compressive strength (MPa) 5 specimens	Phase present * (1 day)
0.95 ± 0.02	0.77 ± 0.10	HA + TTCP+ CaHPO_4 (trace)
1.06 ± 0.01	0.72 ± 0.06	HA + TTCP+ CaHPO_4 (trace)
1.40 ± 0.04	0.90 ± 0.10	HA + TTCP+ CaHPO_4 (trace)
1.53 ± 0.04	1.00 ± 0.09	HA + TTCP+ CaHPO_4 (trace)
1.63 ± 0.01	0.80 ± 0.10	HA + TTCP+ CaHPO_4 (trace)

*The first one was the main phase as shown in Fig. 4.28.

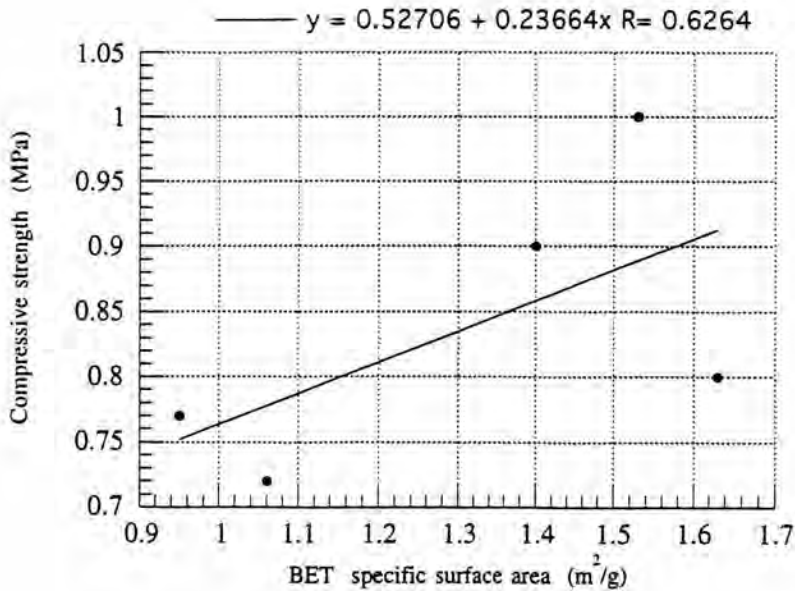


Fig.4.19 Effect of specific surface area of TTCP on the compressive strength of cement added 35 wt% HA.

From Table 4.16 and Fig 4.19, the trend of compressive strength of the cements containing DCPD particle (having diameter of 5–10 μm) was slightly increased with increasing of specific surface area (SS) of TTCP.

Otsuka M. et al. (1993) reported particle size effect of metastable calcium phosphate on crushing strength of calcium phosphate cement. The cement powder consisted of an equimolar mixture of various particle sizes of TTCP (1.1–13.1 μm), and 40 wt% of HA seed crystals. The crushing strength of all cements increased with increasing of the specific surface area of DCPD (small DCPD particles having specific surface area 4.93 m^2/g), and that of the cements containing the smallest TTCP particles (specific surface area = 1.71 m^2/g) was the hardest. At the initial stage of cement setting, the dissolution rate of metastable substance was considered to be diffusion-controlled as shown by the Noyes-Whitney equation :

$$dC/dt = kS / V (C_s - C)$$

Where k was the rate constant per unit area, S was the available

surface area, V was the solvent volume, C_s was the solubility and C was the solute concentration.

The dissolution rate of the metastable form of calcium phosphate was controlled by the solubility and surface area of the solid. Since the solubility of TTCP was higher than that of DCPD, the specific surface area of TTCP affected the compressive strength more than that of DCPD.

Liu et al. (1997) reported the variation of pH with time in CPC slurry. They deduced that the crystals did not occur until the supersaturation was up to a high value by the solution of DCPA and TTCP in the absence of crystals seed, and the presence of crystal seed would reduce the supersaturation to produce HA. Therefore, the presence of seed might lead to the delay of the HA formation.

Table 4.17 Effect of P/L ratio on the compressive strength of cement containing the equimolar mixture of TTCP prepared at 1350°C and DCPD in presence of 35 wt% of HA(70) (SS of TTCP = $1.53 \pm 0.04 \text{ m}^2/\text{g}$, 5 unpressed specimens)

P/L ratio (g/ml)	Compressive strength (MPa)	phase result by X-ray diffraction* (1 day)
1.5	0.4 ± 0.04	HA+TTCP+CAHPO ₄
1.7	0.6 ± 0.02	HA+TTCP+CAHPO ₄
2.0	1.0 ± 0.08	HA+TTCP+CAHPO ₄
2.2	0.7 ± 0.10	HA+TTCP+CAHPO ₄
2.4	0.2 ± 0.09	HA+TTCP+CAHPO ₄

* XRD patterns showed in Fig. 4.29.

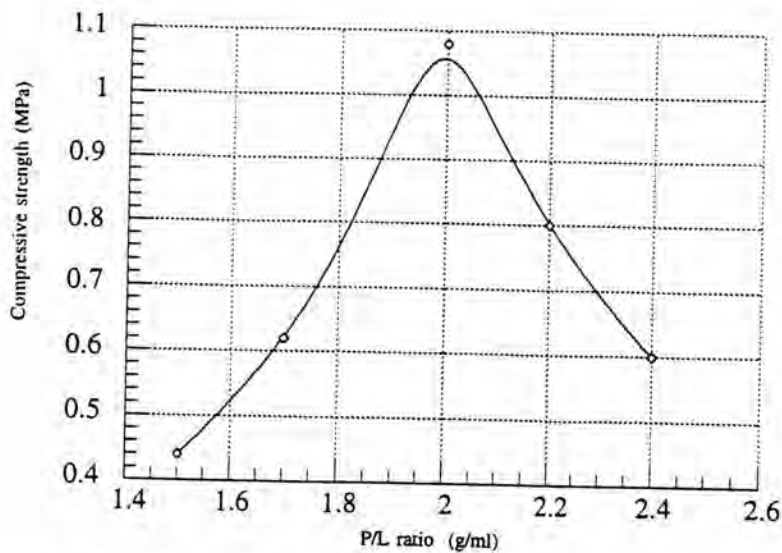


Fig. 4.20 The relationship between P/L ratio of cement pastes added 35 wt% HA(70) and the compressive strength

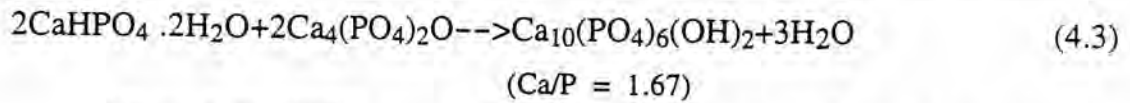
The change of strength with various P/L ratios of cement pastes was shown in Fig.4.20. It was found that in presence of 35wt% of HA(70), the P/L ratio of 2.0 gave the highest compressive strength. However, besides the P/L ratio, strength of cement also depended on other factors, such as cement composition, fineness, curing time, curing temperature, and so on.

Table 4.18 Comparison of compressive strength (MPa) of cements containing the equimolar mixtures of TTCP(1350) and DCPD with that of cement containing the equimolar mixture of TTCP(1350) and DCPA at P/L ratio of 2.0 and 2.4 g/ml, 5 unpressed specimens.(SS of TTCP =1.53 m²/g)

P/L	2.0	2.4
Composition		
TTCP+DCPD+35wt%HA(70)	1.0±0.08*	0.2±0.09*
TTCP+DCPA+35wt%HA(70)	0.4±0.04	0.6±0.02

* results from Table 4.17

The reaction of the equimolar mixture of TTCP and DCPD was as follows :



Chow L.C. (1991) reported that the reaction was also as follows :

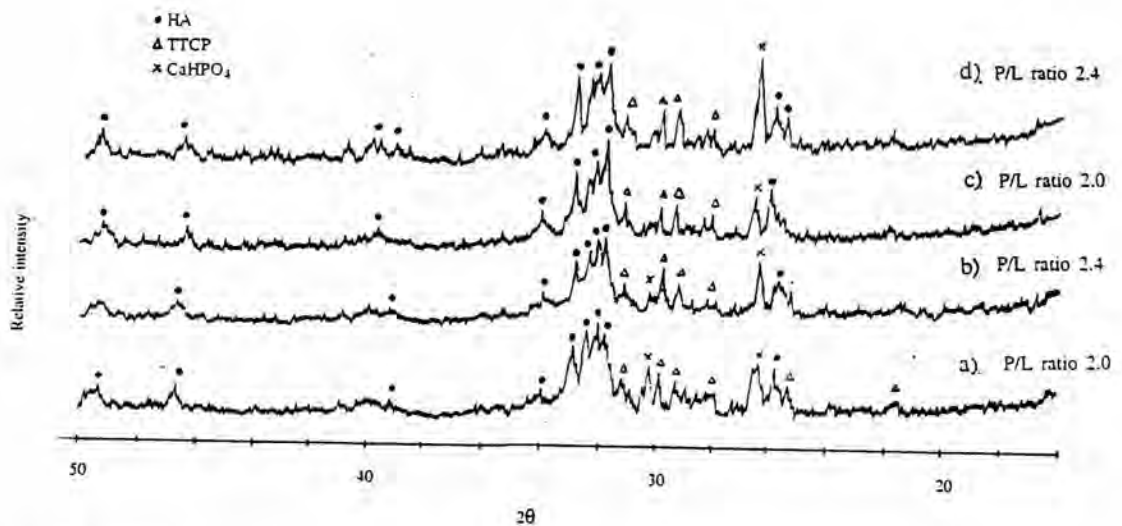
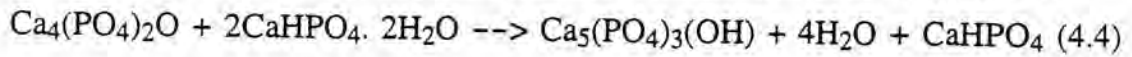


Fig. 4.21 XRD patterns of phase obtained of cement containing TTCP+ DCPD+35 wt% HA (a and b) and TTCP+DCPA+35 wt% HA (c and d). (from Table 4.18)

X-ray diffraction patterns of phase obtained as shown in Fig. 4.21 was HA, residual TTCP and CaHPO_4 .

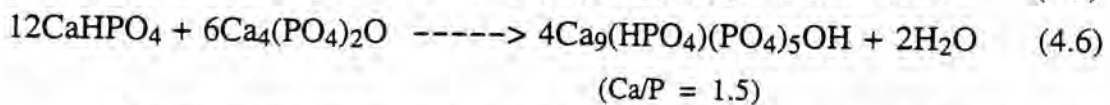
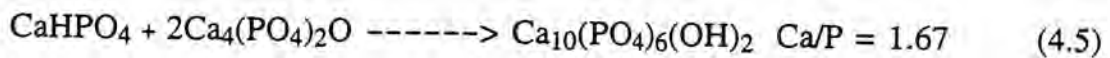
Tung et al. (1985) reported that in the pH range above the singular point between DCPD and HA (pH = 4.3 at 25°C), HA had the lowest solubility of the calcium phosphates that could be formed at 25°C. Therefore thermodynamically, the end-product of DCPD hydrolysis at 25°C in this pH range and in the absence of CaF_2^* should be HA.

* used as additive to promote the reaction.

Sometimes they observed DCPA as a by-product in the lower pH range (6.2–6.8) and in absence of fluoride, because DCPA was more stable than DCPD, and DCPA would not hydrolyze to OCP (octacalcium phosphate) readily. DCPA would hydrolyze to HA at higher pH, higher temperature, or in the presence of fluoride. Therefore, this experiment found that DCPA was a by-product in most of the cases of 1 day cured cements and very few cases that the phase DCPA was absent (Fig. 4.26)

Matrin and Brown (1993) found that the solubility isotherms of $\text{CaHPO}_4 \cdot 2\text{H}_2\text{O}$ (DCPD), CaHPO_4 (DCPA) and the pseudo-isotherm of TTCP crossed at a pH near physiological pH. This intersection involved equilibria between the two solids and the aqueous phase and was, therefore, an invariant point. However, the invariant points between TTCP and DCPD or DCPA were metastable with respect to the solubility isotherm of hydroxyapatite which precipitated under nominally steady-state conditions (eq. 4.3). However, balancing the dissolution rates of the reactants was difficult because of the incongruent dissolution of the acidic constituents and hydroxyapatite nucleation on the precursors. Brown (1992) and Fulmer (1991) found that brushite and monetite both dissolved incongruently and HA nucleated on the surfaces essentially forming a diffusion barrier to their further dissolution.

The reaction of the equimolar mixture of DCPA and TTCP was led to the formation of stoichiometric and calcium-deficient HA had been identified :



The reactions illustrated could be considered in terms of solubilities of the reactants and of HA as illustrated in Fig. 2.5.

In a ternary system at constant temperature and pressure, the intersections of the solubilities curves for DCPA and HA, and for DCPA and

TTCP were invariant or singular point, the intersection of DCPA and HA was a stable invariant point, while that for DCPA and TTCP was metastable : the invariant solution was supersaturated with respect to HA. When the solid DCPA and TTCP dissolve in aqueous solution, the system was driven toward metastable invariance, which was continuously disturbed by HA formation.

Brown. et al. (1991) reported that a steady-state pH did not appear to be reached when the experiment (3 days) was conducted at DCPA:TTCP molar ratio of unity. Analysis of the solids present at the termination of the experiments after 7 days of reaction indicated the presence of both unreacted TTCP and DCPD when their original ratio was unity. This finding was consistent with calcium concentration and the pH data. However, this experiment could not clearly explain mechanism that the formation of HA effected on the compressive strength of cement.

Fig 4.22 showed SEM micrograph of crushed specimens. The microstructure obtained after 1 month of specimens containing hydrated phase mixed with the reactant phase and showed the large pore size.

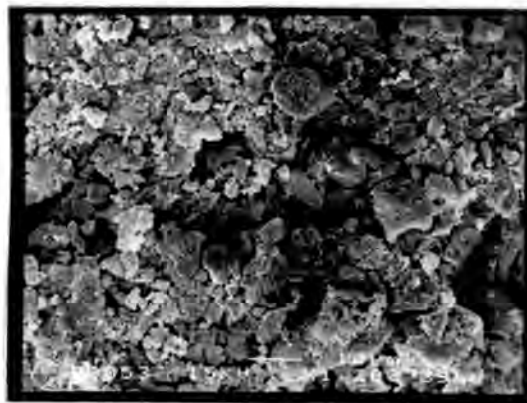
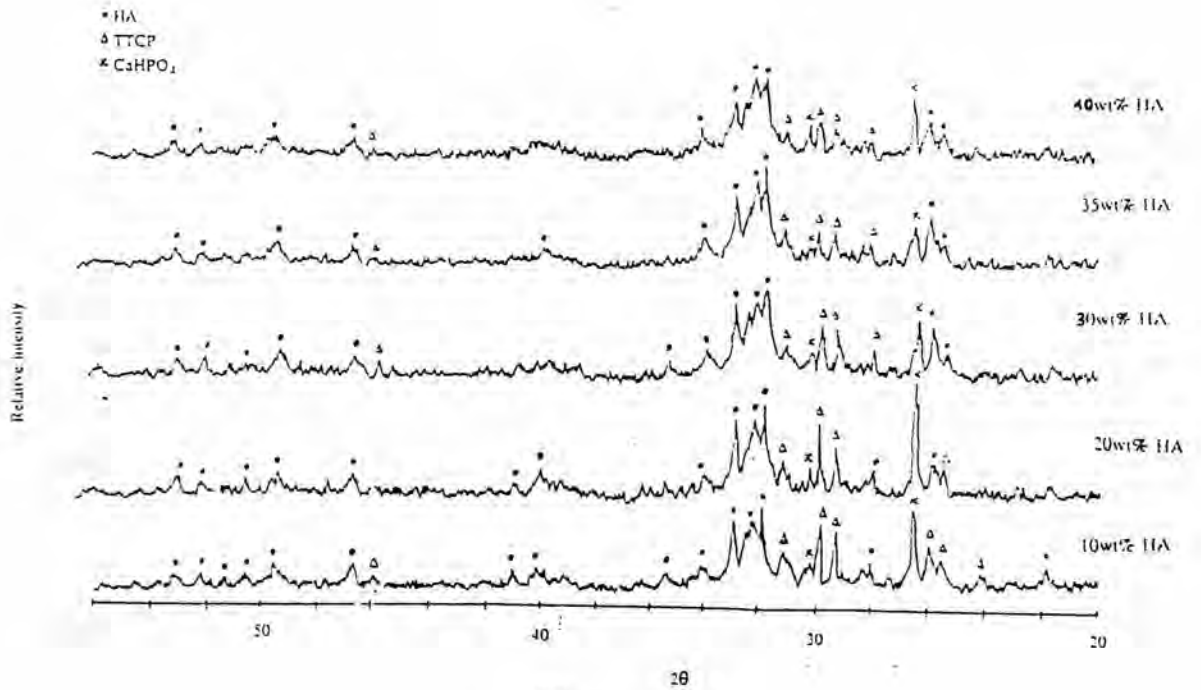
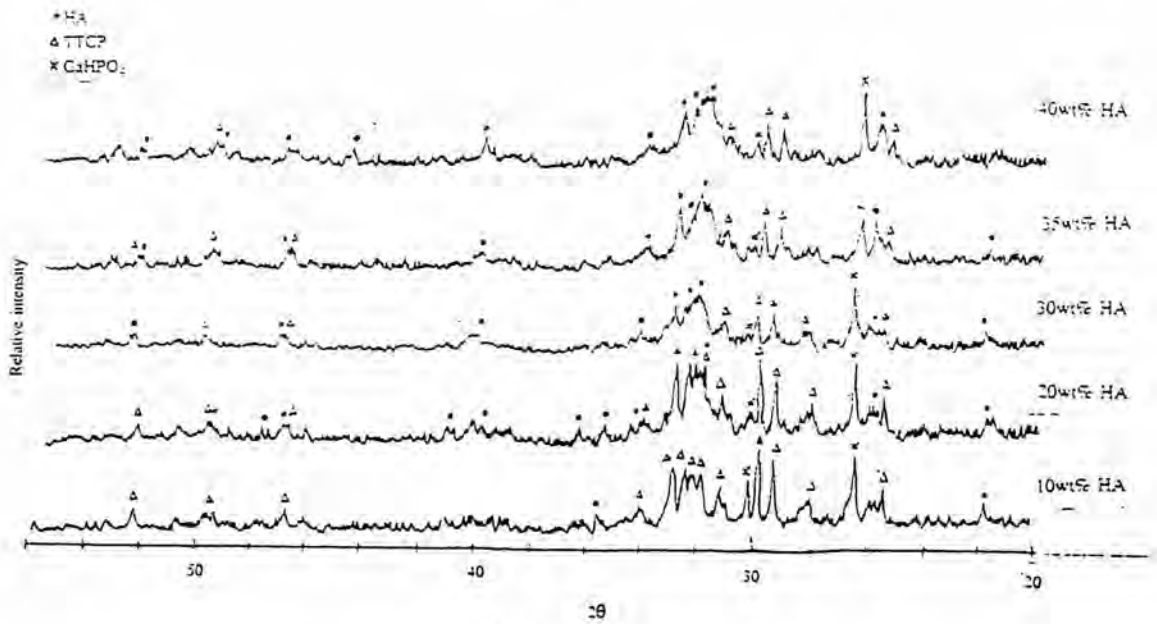


Fig. 4.22 SEM micrograph of crushed specimen containing TTCP(1350)+ DCPD mixture added 35 wt% HA(70), P/L ratio of 2.4 g/ml. (curing 1 month)

c) Phase of cements.



(a)



(b)

Fig. 4.23 XRD patterns of cements containing: (a) TTCP(1350) and DCPD and (b) TTCP(1400) and DCPD in presence of various contents of HA(70) at P/L ratio of 2.0 g/ml.

Fig. 4.23 showed that the formation of HA phase as hydration product increased with the increase of HA(70) content as seed in both cements containing TTCP(1350) and TTCP(1400).

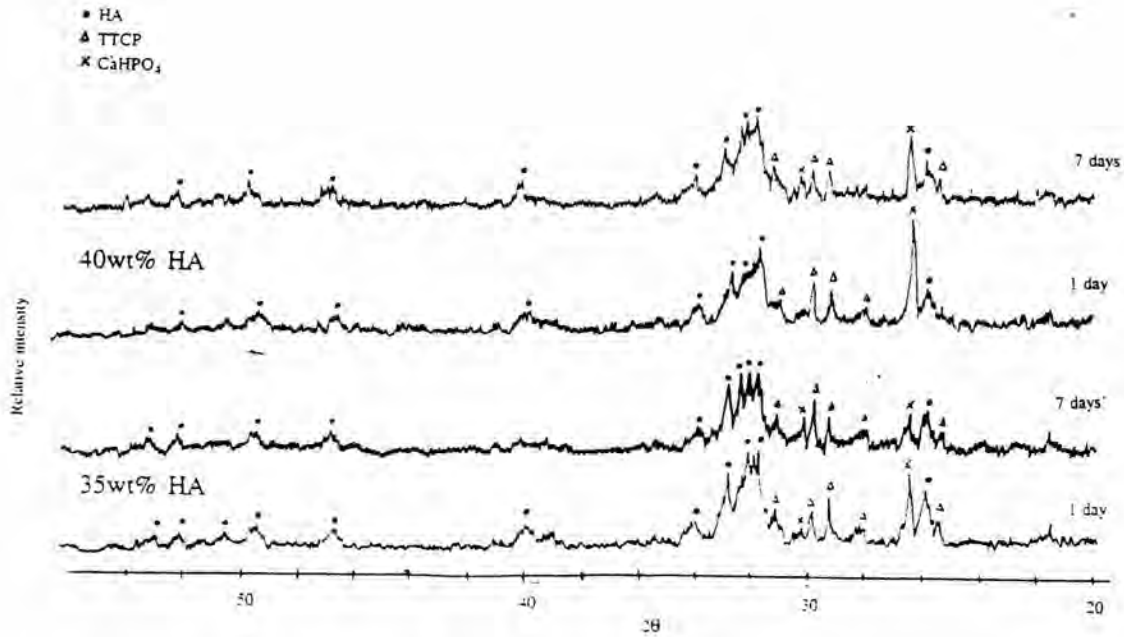


Fig. 4.24 XRD patterns of cement containing the equimolar mixture of TTCP(1350°C) and DCPD in presence of 35, 40 wt% HA(70) at P/L ratio of 2.0 g/ml for 1 and 7 day curings.

Results from Fig. 4.24 showed that HA, unreacted TTCP and CaHPO₄ were the phases found at 1 and 7 day curings.

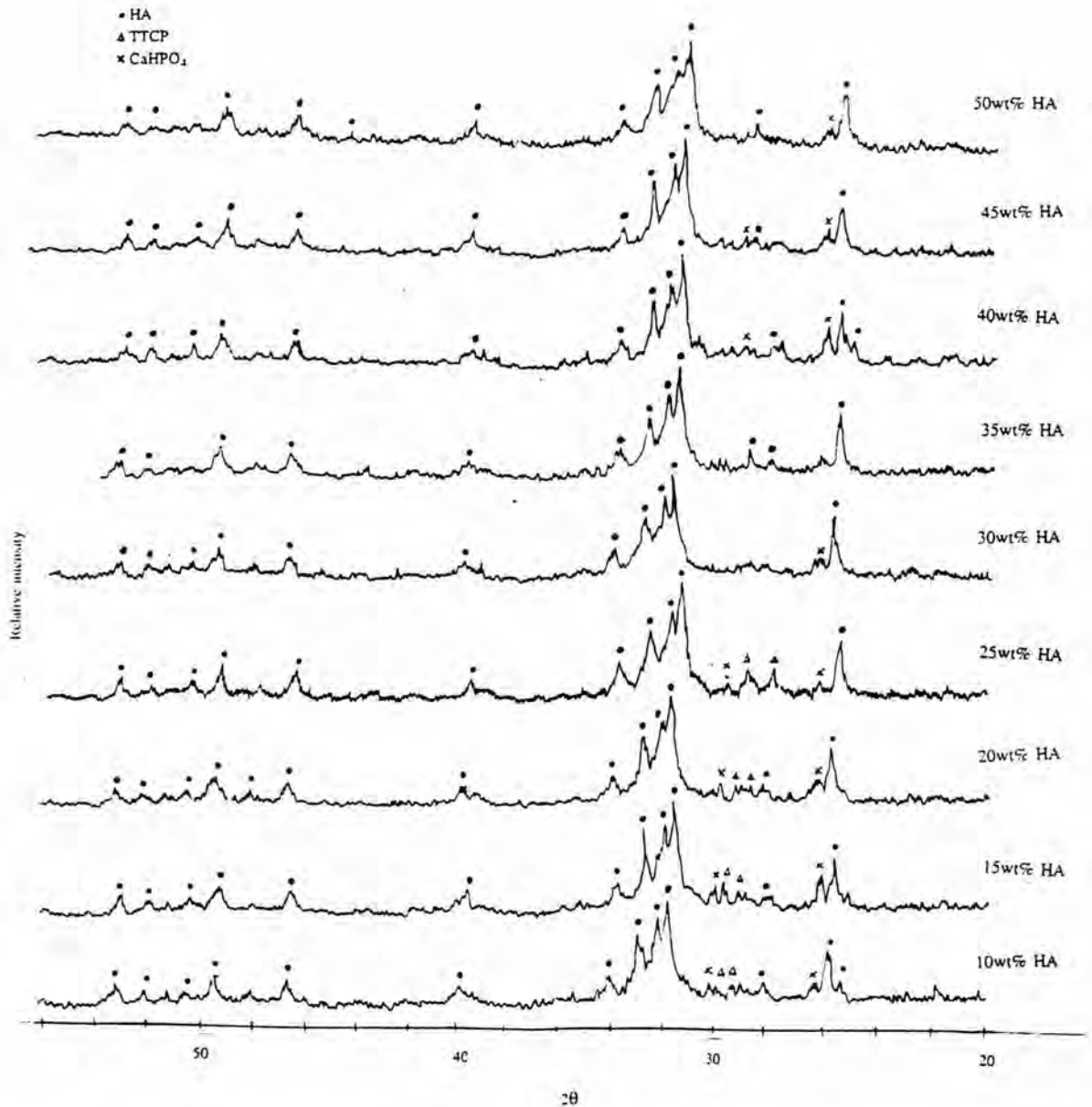
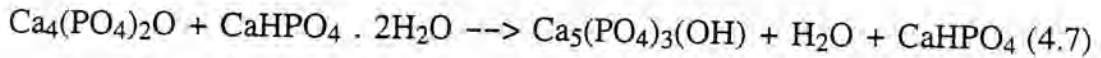


Fig 4.25 Phases obtained from cements containing the equimolar mixture of TTCP(1350°C) and DCPD with various contents of HA(70) at P/L = 1.7 g/ml (curing for 1 month)

Fig. 4.25, shows XRD patterns of phases obtained after 1 month. Phases obtained after 1 day (Fig. 4.23) were HA, residual TTCP and CaHPO₄ ($d = 3.37, 2.96$) which were in accordance with the patent of Brown and Chow (1988) : a process of preparing Ca-P cement by the following reaction :



However, in this experiment the reaction at 1 day could not occur completely because specimens were not stored at 100% humidity. Thus, residual TTCP also remained (Fig. 3.19 desiccator modified for curing the specimens having $80 \pm 10\%$ humidity). The longer curing could lead to complete reaction as shown in samples curing for 1 month (Fig. 4.25) whereas nearly no trace of TTCP was left.

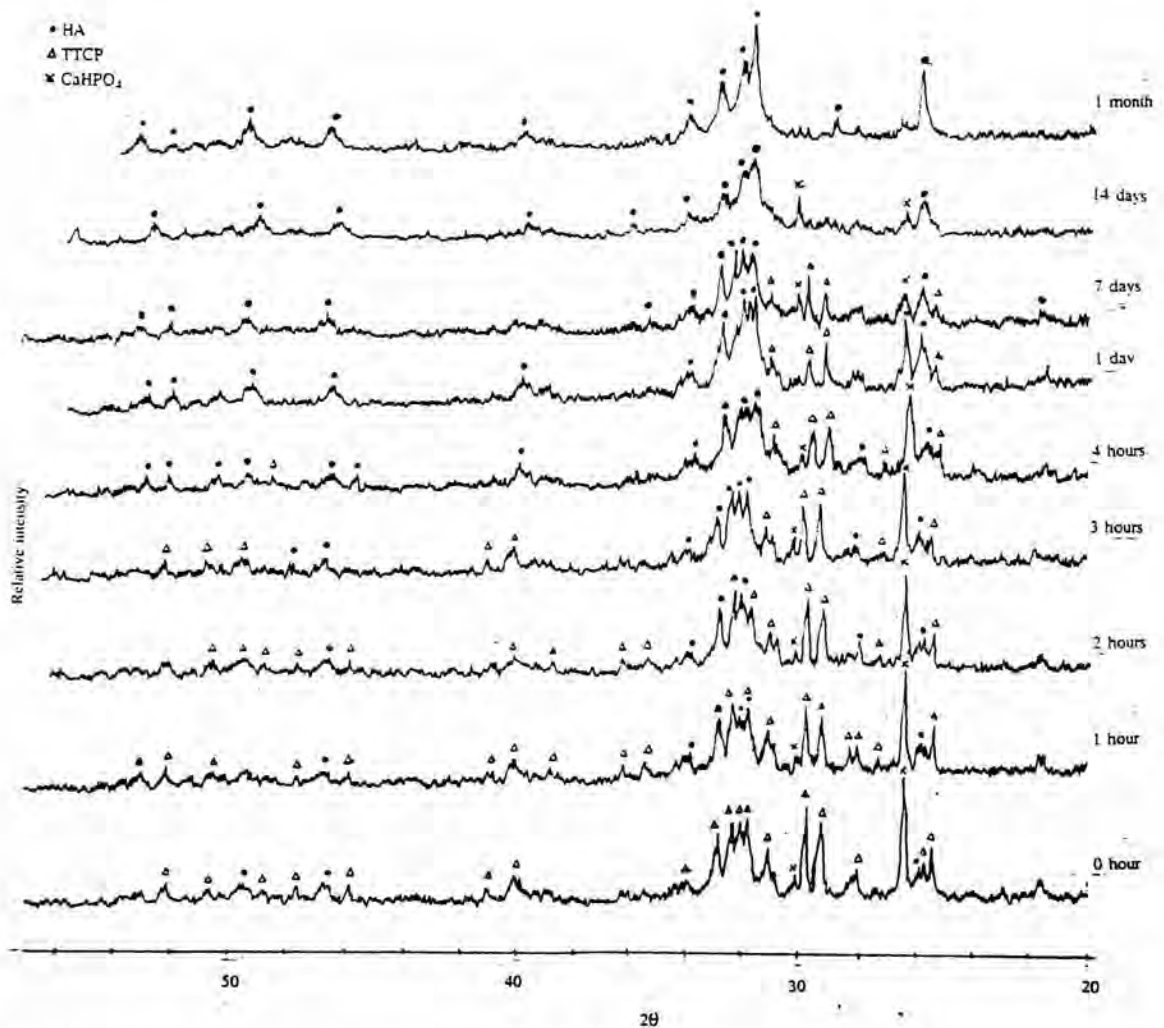


Fig. 4.26 XRD patterns of hydrated specimens [TTCP(1350)+DCPD+35 wt% HA(70)] obtained at different curing times.

Fig. 4.26 showed that the final product was HA. HA increased with curing time as expected but x-ray diffraction also detected unreacted TTCP and DCPA at 7 days curing and only HA was observed at 1 month.

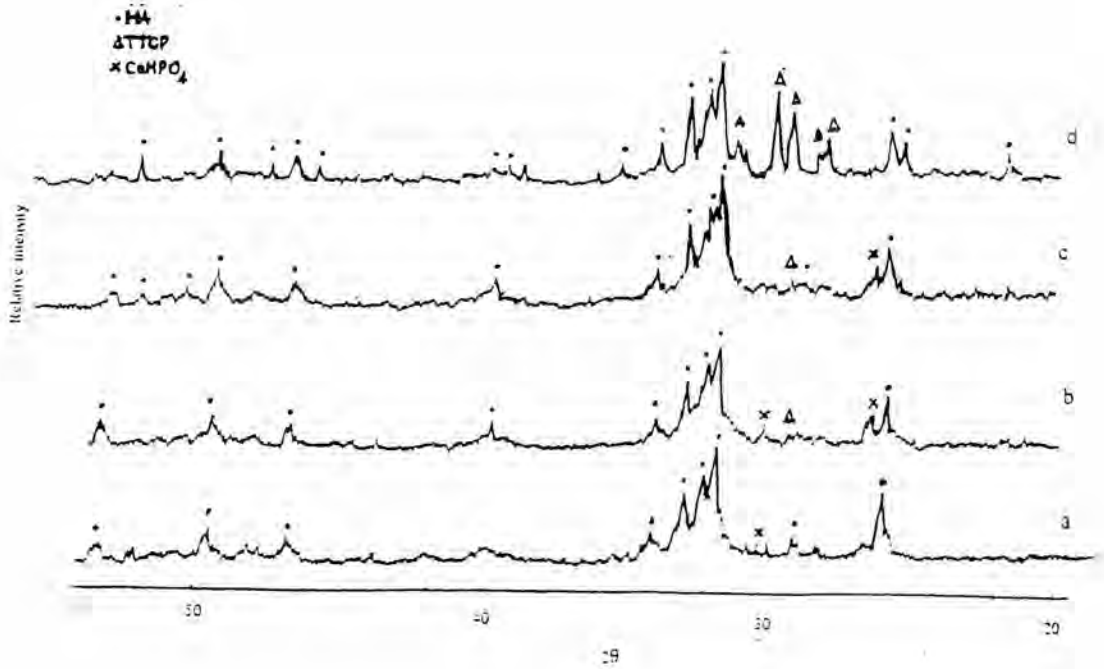


Fig. 4.27 XRD patterns of phase obtained of cement added 35wt% HA(70) :
 a) sieved (-325#), b) unsieved and
 added 45wt% HA : c) sieved (-325#), d) unsieved

Fig. 4.27, showed effect of particle size of HA(70) as seed on hydration of cement when 35 wt% and 45 wt% of (-325#) HA(70) were added in the mixture of CPC powder, after 1 day hydration, conversion of TTCP to HA was better than that of unsieved HA(70).

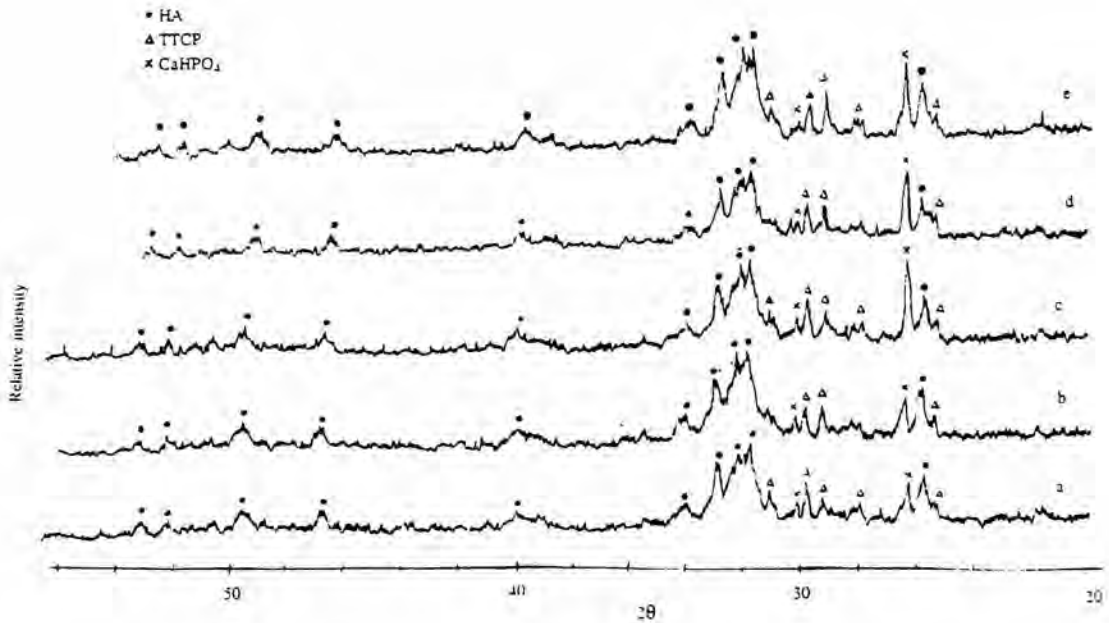


Fig. 4.28 Shows X-ray patterns of cements containing TTCP having various specific surface areas. : a) SS 0.95, b) SS 1.06, c) SS 1.40, d) SS 1.53, e) SS 1.63 m²/g.

Results of Fig. 4.28 indicated that phases obtained after 1 day curing of all the cement specimens were HA, residual TTCP and CaHPO₄. However, there was only a slight difference among the XRD patterns in Fig. 4.28, therefore the effect of specific surface area of TTCP upon the extent of hydration reaction could not be drawn. This might be due to the too narrow range of the specific surface area used for the experiment.

Phases obtained after mixing 1 day of cement containing 35 wt% of HA at various P/L ratios were HA, residual TTCP and little amount of CaHPO₄ as shown in Fig. 4.29.

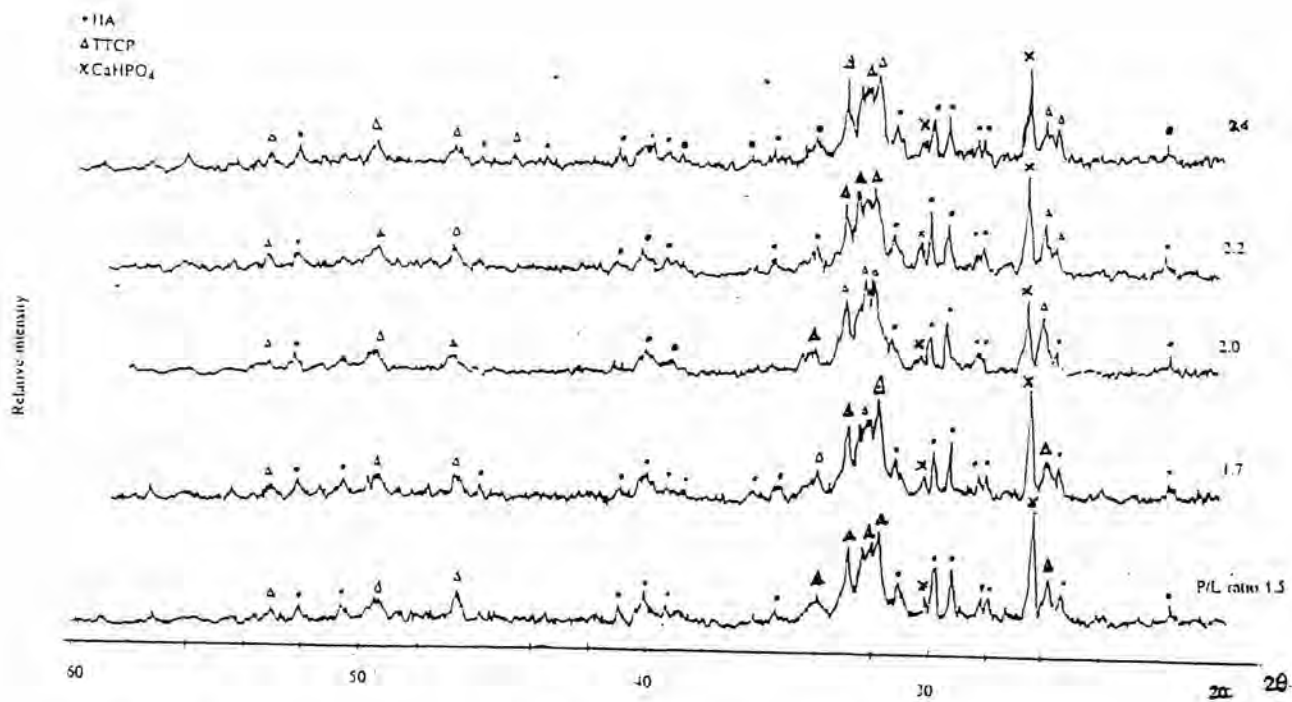


Fig. 4.29 XRD patterns of cement (SS of TTCP = $1.63 \text{ m}^2/\text{g}$) containing 35 wt% HA as seed at various P/L ratios after 1 day curing.